(Received 19 October 2023, Accepted 23 January 2024, Scheduled 18 February 2024)

Improved Skew Method in Permanent Magnet Motor with Segmented Rotors for Reducing Cogging Torque

Sizhan Hua[1], Xueyi Zhang[1,*], Jun Zhang[2], Chenglong Yu[3], Fanxi Meng[4], Wei Wang[1], Kai Geng[1], and Wenjing Hu[1]

[1]*Shandong University of Technology, School of Transportation and Vehicle Engineering, Zibo 255000, China*
[2]*Shandong Tangjun Ouling Automobile Manufacturing Co. Ltd, Zibo 255000, China*
[3]*Zibo Yongtai Motor Co. Ltd, Zibo 255000, China*
[4]*Shandong Bentu New Energy Vehicle Industry Co. Ltd, Taian 271000, China*

ABSTRACT: Rotor segment skew pole can effectively weaken the cogging torque, but the traditional rotor segment skew pole can also cause the unbalanced axial electromagnetic force, then add load to the bearing thus affecting the performance and decreasing the service life of the motor. It is complicated to study the effect of segment skew pole by the energy method. According to the generating mechanism of cogging torque, this paper presents an easy method. The relationship between rotor segment number and cogging torque harmonics weakening is analysed through the application of geometrical relation and Fourier series, and a simple method for determining segment number is obtained. By analysing the main source of axial force in rotor segment, a new type of rotor arrangement is proposed, which can avoid excessive axial force while retaining the effect of traditional skew mode on cogging torque weakening. The correctness of the conclusion is verified by finite element simulation and prototype experiment.

1. INTRODUCTION

The permanent magnet motor has the advantages of high efficiency, high energy density, simple control, and easy maintenance. It is widely used in various household appliances, vehicles, high-tech equipment, advanced manufacturing and new energy industries [1, 2]. However, the unique cogging torque phenomenon of permanent magnet motor limits its application in high precision control, silent drive, etc. [3]. Compared with fractional slot [4, 5], the harmonic spectrum of the armature winding of the integer slot motor is sparser than that of the fractional slot motor, which can effectively reduce the radial electromagnetic force, obtain a better NVH performance [6, 7], but the cogging torque of the integer slot motor is larger. The methods to reduce the cogging torque include optimizing the pole arc coefficient [8], different slot widths [9], rotor slotting [10], etc. Methods like stator skew [11] or rotor segment skew poles [12–14] prove effective in suppressing cogging torque and electromagnetic noise [15, 16]. However, they introduce unbalanced axial magnetic tension [17], causing additional load on the bearings and axial movement of the motor [18]. Thus, reducing cogging torque while avoiding axial force has become a crucial research focus for permanent magnet motors.

Scholars predominantly employ energy methods [19–23], which reveals the origins of the cogging torque and provides valuable guidance for its reduction. In 2002, Zhu and Howe studied the simple influential laws of optimization design parameters such as pole and slot combination, pole arc coefficient, and skew angle about the cogging torque [24]. However, the derivation and explanation of these formulas were not provided. In 2009, Zhu's team used energy method and Fourier series analysis to formulate the general analytical expression for cogging torque [25]. Based on the condition that the energy storage of the air gap magnetic field is not zero, the relationship between the period of cogging torque and the combination of pole and slot was derived. The optimal design parameters such as pole and slot combination, skew angle of slot, pole arc coefficient, and stator slot opening were identified. These parameters hold significant theoretical guidance for minimizing cogging torque. Reza and Srivastava introduce a method for reducing cogging torque through the skewing of slot openings. This novel approach presents a noteworthy path for further investigation and potential implementation in motor design optimization. But for motors with a large number of stator slots and small openings, this method is difficult to apply [26]. In terms of stator skew and rotor segment skew pole, Baolai analysed the axial force expression caused by the skew [27] and misalignment in stator and rotor axes. Lipo's team proposed a sinusoidal segmented skew pole structure [28] that avoids axial force through axial symmetry arrangement. However, applying this method to motors with a small radial length ratio and numerous segments is challenging. Lin et al. [29] from Shanghai University delved into rotor segment number and skew pole arrangement (linear skew pole, cross skew pole, V antisymmetric skew pole structure, etc.), They suggested that magnetic leakage between two adjacent rotated segments of permanent magnet rotor is the primary cause of unbalanced axial force. Among the various arrangements, cross-skew pole and V shape antisymmetric skew pole were found to have less weakening effect on cogging torque than linear skew poles, under the same number of segments. This paper deviates from complex energy

* Corresponding author: Xueyi Zhang (zhangxueyi@sdut.edu.cn).

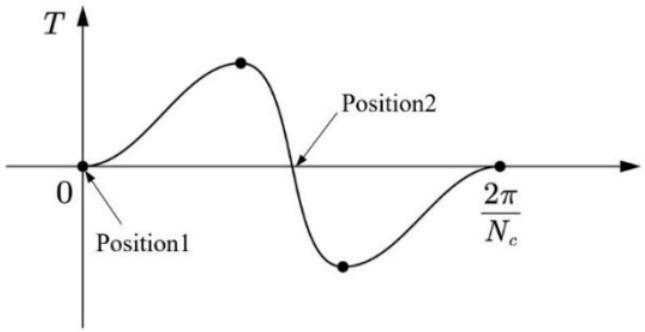

FIGURE 1. Typical cogging torque wave form.

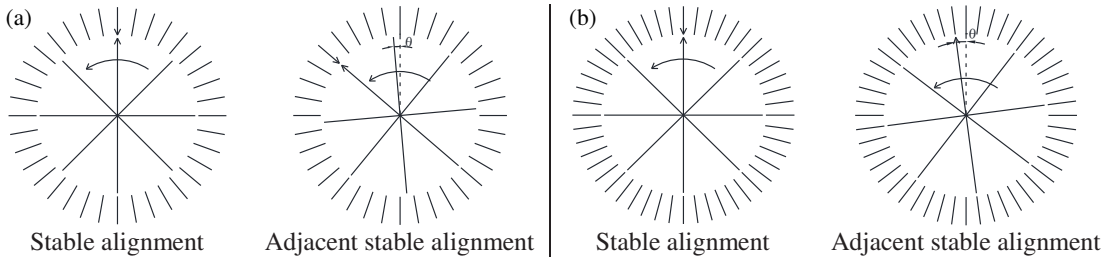

FIGURE 2. Relation between rotor position and stable alignment angle. (a) 8 poles-36 slots. (b) 8 poles-48 slots.

methods, focusing on the mechanical characteristics of cogging torque. It deduces the weakening effect of a uniformly linear step skew pole on cogging torque harmonics, establishes the relationship between the number of segments and harmonic order, and proposes a novel rotor segment arrangement method. The validity of this proposed arrangement is confirmed through finite element modelling of an 8-pole 48-slot motor.

2. MATHEMATICAL DERIVATION OF THE COGGING TORQUE PERIOD

Before delving into the details of the proposed method, it is essential to establish a necessary assumption: both the rotor pole and stator slot are assumed to be symmetrical and evenly distributed.

The process of calculating the cogging torque period using energy method is complicated. Instead, this paper proposes a method, which simplifies the process by deducing the cogging torque period based on the typical cogging torque waveform. This involves extracting the geometrical relationship embedded in the mechanical characteristics of the cogging torque. The cogging torque is caused by the stator slotting; the rotor produces torque because it always tends to maintain at some specific positions in static states. Figure 1 illustrates a typical cogging torque diagram [24], providing a visual representation

The cogging torque is observed to be zero under the following positions:

1. The centerline of the rotor poles is aligned with the center of the stator teeth;

2. The centerline of the rotor poles is aligned with the center of the stator slots.

Position 1 is identified as a stable state while position 2 is not. Therefore, we define the stable state of position 1 as "stable alignment". In the rotation process of the rotor, the minimum angle that needs to be rotated for two adjacent stable alignment is called the alignment angle θ (as shown in Figure 2). This mechanical angle corresponds to one cycle of cogging torque. The number of times that stable alignment occurs within one revolution of the rotor corresponds to the frequency of cogging torque.

Since the magnitude and period of the cogging torque are independent from the motor's rotation direction, the relationship between the stable alignment angle and the combination of poles and slots can be expressed as:

$$\theta = \min \left| k\frac{2\pi}{N_s} - m\frac{2\pi}{N_p} \right|, \quad k, m \subset N_+ \tag{1}$$

where N_s is the number of stator slots, and N_p is the number of rotor poles $\theta \neq 0$. Then, as the rotor completes one cycle, the number of periods in which the cogging torque changes is $N_c = 2\pi/\theta$. Substituting θ into Equation (1), we get:

$$N_c = \frac{N_s N_p}{\min |kN_p - mN_s|} \tag{2}$$

Extract the greatest common divisor of the two numbers. As there must be a solution where the linear combination of the two mutually prime numbers has a value of 1, the cogging torque period is expressed as:

$$N_c = \frac{N_s N_p}{GCD\,(N_s, N_p) \cdot 1} = LCM\,(N_s, N_p) \tag{3}$$

where *GCD* represents the greatest common divisor of N_s and N_p, and *LCM* represents the least common multiple of N_s and N_p.

3. COGGING TORQUE WITH STATOR SLOT SKEW OR ROTOR POLE STEP SKEW

3.1. Mathematical Derivation

The cogging torque waveform manifests an oddly symmetrical figure, which can be expressed in the form of a Fourier series as below (same as the expression of cogging torque in [30] by Ge et al.)

$$T_{unskew}(\alpha) = \sum_{n=1}^{\infty} T_n \sin(nN_c\alpha) \tag{4}$$

where T_n represents the amplitude of the harmonic order n, and α represents the rotor position. Assume that the rotor is uniformly linear step skewed. The expression of cogging torque for a rotor with a linear step skew pole of total angle β has the following form:

$$T_{stepskew}(\alpha) = \sum_{i=1}^{j}\sum_{n=1}^{\infty} \frac{T_n}{j} \sin\left[nN_c(\alpha - \frac{i}{j}\beta)\right] \tag{5}$$

where j represents the total number of segments, and i represents the segment serial number. When the number of segments tends to infinity, this formula can also represent the cogging torque of the stator slot skew of total angle β, that is:

$$\begin{aligned} T_{conskew}(\alpha) &= \lim_{j\to\infty} \sum_{i=1}^{j}\sum_{n=1}^{\infty} \frac{T_n}{j} \sin\left[nN_c(\alpha - \frac{i}{j}\beta)\right] \\ &= \sum_{n=1}^{\infty} T_n \int_0^1 \sin\left[nN_c(\alpha - x\beta)\right] dx \\ &= \sum_{n=1}^{\infty} \frac{T_n}{n} \left\{\cos\left[nN_c(\alpha-\beta)\right] - \cos(nN_c\alpha)\right\} \end{aligned} \tag{6}$$

As can be seen from the above formula, when $\beta = k\frac{2\pi}{N_c}, k \subset N_+$ (which means integer multiples of one cogging torque mechanical period angle θ), the cogging torque is weakened to 0 (When the stator slot skew method is used, $k = 1$ is usually taken to reduce the unbalanced axial electromagnetic force caused by the skew [31]). However, because the stator and rotor of the motor are made of silicon steel sheet superimposed, the number of segments is limited and affected by the machine manufacturing accuracy, the eccentric of stator and rotor, etc. The cogging torque value cannot be reduced to zero. Due to the increased producing difficulty of the stator slot skew method and the difficulty of wire embedding, its applications are not as many as those of the rotor segment skew method.

As for the rotor segment skew pole, since the cogging torque is independent of the direction of the skew pole, its expression can also be expressed as:

$$\begin{aligned} T_{stepskew}(\alpha) &= \sum_{i=1}^{j}\sum_{n=1}^{\infty} \frac{T_n}{j} \sin\left[nN_c(\alpha - \frac{i}{j}\beta)\right] \\ &= \sum_{i=1}^{j}\sum_{n=1}^{\infty} \frac{T_n}{j} \sin\left[nN_c(\alpha + \frac{i}{j}\beta)\right] \end{aligned} \tag{7}$$

Expand and organize the above formula to obtain:

$$T_{stepskew}(\alpha) = \sum_{i=1}^{j}\sum_{n=1}^{\infty} \frac{T_n}{j} \sin(nN_c\alpha)\cos\left(nN_c\frac{i}{j}\beta\right) \tag{8}$$

It can be seen that the determination of the optimum number of segments and the angle of the skew pole is related to the amplitude of each harmonic. Similar to the stator slot skew method, $\beta = \frac{2\pi}{N_c}$ was taken to avoid excessive unbalanced axial force. The relationship between the number of segments and the weakening of the cogging torque is now simplified as bellow:

$$T_{stepskew}(\alpha) = \sum_{i=1}^{j}\sum_{n=1}^{\infty} \frac{T_n}{j} \sin(nN_c\alpha)\cos\frac{2\pi ni}{j} \tag{9}$$

Equation (9) can be simplified based on the number of $\sum_{i=1}^{j} \cos\frac{2\pi ni}{j}$:

1. When the harmonic number n is an integer multiple of the total segment number j:

$$\sum_{i=1}^{j} \cos\frac{2\pi ni}{j} = j \tag{10}$$

Substitute Equation (10) into Equation (9), and compare with Equation (4) to get:

$$stepskewT_{kj} = unskewT_{kj}, \quad k \subset N_+ \tag{11}$$

2. When the harmonic order n is not an integer multiple of the total segment number j, according to the summation formula (mathematically, this summation formula is derived from Euler's formula):

$$\begin{aligned} \sum_{i=1}^{j} \cos\frac{2\pi ni}{j} &= \frac{\sin(j+\frac{1}{2})\frac{2\pi n}{j} - \sin\frac{1}{2}\frac{2\pi n}{j}}{\frac{1}{2}\sin\frac{1}{2}\frac{2\pi n}{j}} \\ &= \frac{\sin(2\pi n + \frac{\pi n}{j}) - \sin\frac{\pi n}{j}}{\frac{1}{2}\sin\frac{\pi n}{j}} = 0 \end{aligned} \tag{12}$$

According to Equations (11) and (12), the cogging torque expression for the uniform linear step skew pole with segment number j is as follows:

$$T_{stepskew}(\alpha) = \sum_{k=1}^{\infty} T_{kj} \sin(kjN_c\alpha) \tag{13}$$

TABLE 1. Relationship of segments and harmonic orders.

Total Segment number	Harmonic order									
	1	2	3	4	5	6	7	8	9	1
1	T_1	T_2	T_3	T_4	T_5	T_6	T_7	T_8	T_9	T_{10}
2		T_2		T_4		T_6		T_8		
3			T_3			T_6			T_9	
4				T_4				T_8		
5					T_5					T_{10}

TABLE 2. Main parameters of prototype.

parameters	value	parameters	value
Rotor poles	8	Gap diameter/mm	95
Stator slots	48	Yoke diameter/mm	140
Rated Torque/Nm	16	PM thickness/mm	4
Rated Power/kW	5	PM length/mm	12
Rated Speed/rpm	3000	Axial length/mm	60
Rated Voltage/V	72	Air gap/mm	0.5

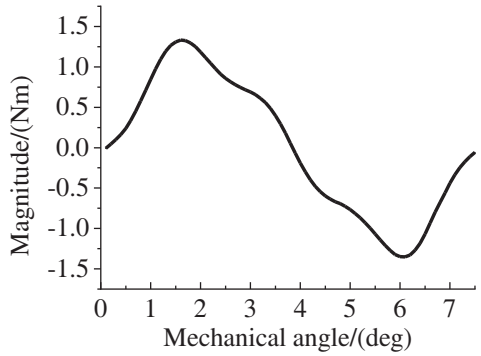

FIGURE 3. Cogging torque wave form.

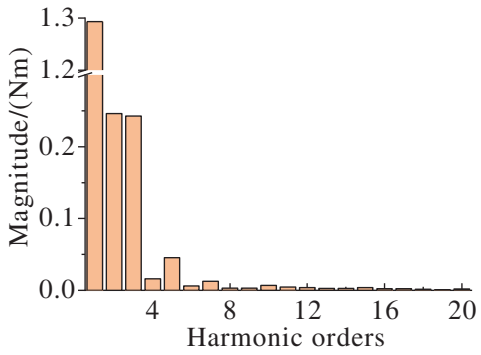

FIGURE 4. Amplitude of first 20th orders.

Equation (13) represents the weakening relationship between the total number of segments and the harmonic order of the cogging torque. That is, when the harmonic order is an integer multiple of the total number of segments, the harmonic amplitude of this order remains unchanged. The harmonic amplitudes of the remaining orders are reduced to zero. (see Table 1).

3.2. Simulate Verification

One simple method to select the initial segment number from above result: Given that the preceding derivation solely relies on the assumption of the basic cogging torque waveform and necessitates symmetry and even distribution of rotor poles and stator slots (an assumption satisfied by the majority of rotating motors). Consequently, this analytical approach exhibits broad applicability. The cogging torque wave form can be obtained through simulation or experimentation, enabling the analysis of harmonic amplitudes using Fourier decomposition to select the optimal number of segments. This methodology provides a convenient means to streamline the design process.

To validate the accuracy of the above conclusion, the finite element method is employed. A two-dimensional finite element model of a V shape permanent magnet synchronous motor (with basic parameters listed in Table 2) is established to analyse the harmonic amplitudes of the cogging torque when the rotor is not segmented.

The cogging torque waveform diagram and the amplitude distribution of each harmonic are presented in Figures 3 and 4. From the distribution of each harmonic amplitude, it can be seen that:

1. The amplitude of the fourth harmonic is less than that of the fifth harmonic;

2. Higher-order harmonics, exceeding the fourth harmonic, exhibit smaller amplitudes than the first four harmonics.

Consequently when using the uniformly segmented step skew pole method to weaken the cogging torque, the cogging torque ripple with the segment number of 4 is superposition of the 4th harmonic and multiples of 4th, primarily influenced by the amplitude of the 4th and a same pattern when the segment number is 5. Therefore, the cogging torque is expected to be less with 4 segments, compared with 5 segments. (Note: This observation is specific to the cogging torque waveform under consideration, but this method applies to other waveforms).

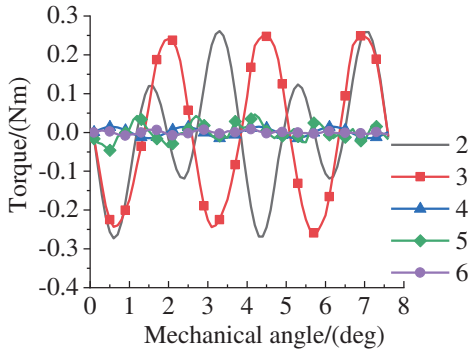

FIGURE 5. Cogging torque by segment number.

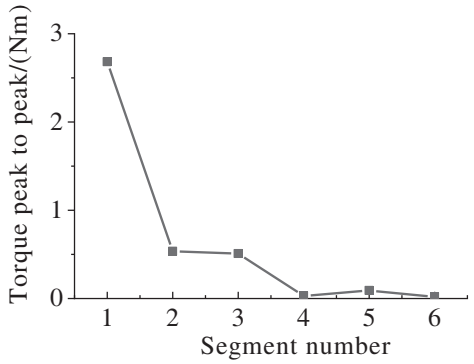

FIGURE 6. Peak difference by segment number.

Two-dimensional parametric modelling was carried out on the segment number, and set the total skew pole angle $\beta = \frac{2\pi}{N_c}$. The skew pole angle between two adjacent segments was $\alpha = \frac{(j-1)\beta}{j}$. Peak difference at different segment numbers of the cogging torque waveform is obtained, as shown in Figures 5 and 6 (The amplitudes of higher harmonics are close to zero, therefore not shown).

It can be seen from Figures 4 and 6, the peak difference of cogging torque under different segments has a similar appearance to the variation of each harmonic amplitude without segments, which reflects the rationality of the above segmented number selection method.

4. SEGMENT INTERCHANGED STRUCTURE

In this paper, a segment interchanged pole structure is proposed to adjust the position of each segment of the traditional linear step skew, so that it retains the weakening effect of the traditional skew pole method on the cogging torque while minimizing the unbalanced axial force as much as possible. According to Maxwell tensor method, the axial force in a permanent magnet motor [32] can be expressed as:

$$\mathrm{F}_z = \frac{1}{\mu_0}\left(\int\limits_{S_1+S_3} \frac{B_z^2 - B_\theta^2 - B_r^2}{2} ds + \int\limits_{S_2} \frac{B_z B_r}{2} ds\right) \quad (14)$$

where F_z is the axial force; μ_0 is the vacuum permeability; B_z, B_r, B_θ are the axial, radial, and tangential magnetic flux densities in the motor, respectively; S_1, S_3 are two axial end faces of the motor; S_2 is the air gap surface of the motor.

When the rotor pole is non-skewed, the axial magnetic forces on two end surfaces are equal in magnitude but opposite in direction. Also, the air gap surface is symmetrical, and the axial resultant force is zero. In the case of a linear step skew pole, the magnetic flux distributions on the two end surfaces are asymmetric at the axial direction. The leakage flux effects of each displaced surface on the air gap surface are superimposed, and the axial force increases with the increase of the total skew angle.

According to the previous analysis, the cogging torque mechanical angular period of the 8-pole 48-slot motor is 7.5 degrees. Under different numbers of segments and different types of skew, the rotation angle of the i-th segment is listed at Table 3.

As shown in Figure 7 and Table 3, the angle between the leakage magnetic fields at two axial ends of the linear step skew pole rotor structure is $\alpha(j-1)$, and the angle between each two segments is α. The superposition of these angles leads to an unbalanced axial force. There is no angle between the two axial ends of the V-shaped skew pole structure, and the internal skew directions are opposite, so the axial force is greatly avoided, but the number of segments is doubled to obtain the same cogging torque reduction effect as the linear step skew structure. Based on the traditional linear step skew pole, half of the skewed segments are interchanged in the structure proposed in this paper. This arrangement maintains the same number of segments of the traditional linear step skew, so it has almost the same weakening effect on the cogging torque. The angle between the magnetic leakage fields at two ends of the axial axis is only α. The unbalanced magnetic force generated by the two ends is smaller than the linear step skew, and the displacement angle of the major shifted face is equal to the sum of the displacement angles between other segments, so the axial forces can partially cancel each other.

In order to verify the above conjectures, 3D finite element simulation models for the 2D structure mentioned above was established. In order to demonstrate the characteristics of the radial air gap and shifted faces magnetic density, the number of segments is set as 3, and each two segments are rotated 2.5 deg initially. The radial air gap magnetic densities of non-skew pole, V shape skew, linear step skew pole, and interchanged skew pole are shown in Figure 8.

It can be seen from Figure 8 that the magnetic field distributions at two ends of the axis vary for different rotor types. According to Formula (14), the axial force after the rotor segment skew pole is also related to the magnitude and direction of the axial magnetic density of the air gap surface. Therefore, the axial magnetic density distribution on the shifted face is analysed. The axial magnetic leakage distribution near the air gap surface [30] of the three skew modes is shown in Figure 9.

In the case of linear step skew, the axial magnetic density and direction between the two adjacent shifted faces are basically the same. Between the shifted faces in opposite directions in the V shape skewed, the axial magnetic density is generally the same but with opposite directions. As the skew pole is interchanged in segments, the axial magnetic density of the major shifted face is the largest, and the axial magnetic density di-

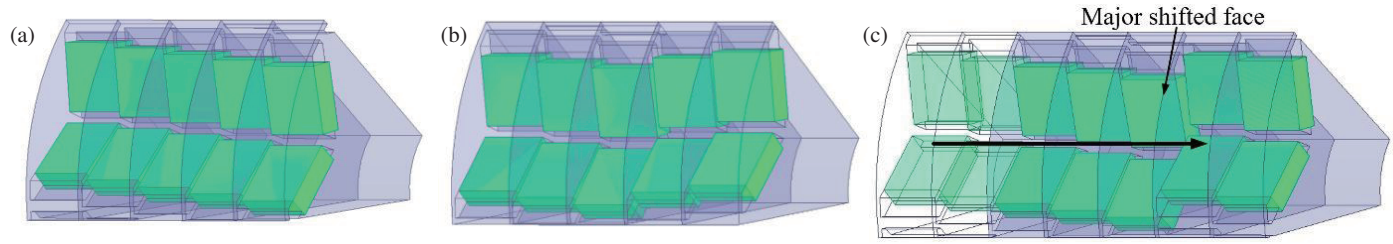

FIGURE 7. Different skew modes. (a) Linear step skew, (b) V shape skew, (c) Interchanged skew.

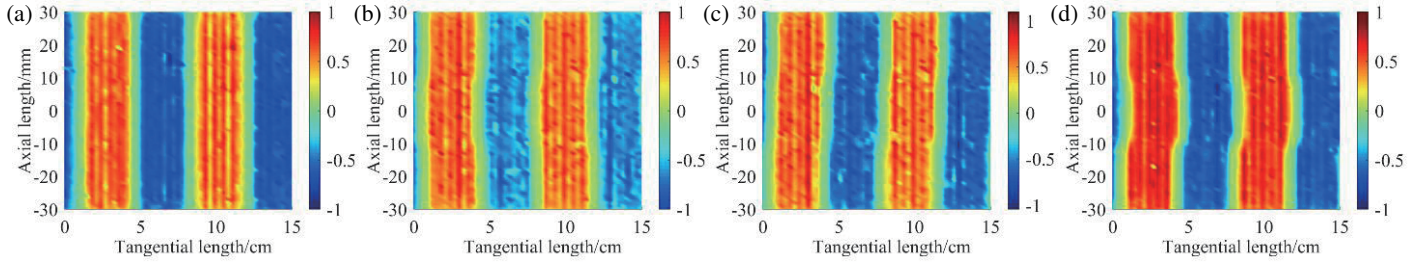

FIGURE 8. Radial magnetic density map. (a) Non-skew. (b) V shape skew. (c) Linear step skew. (d) Interchanged skew.

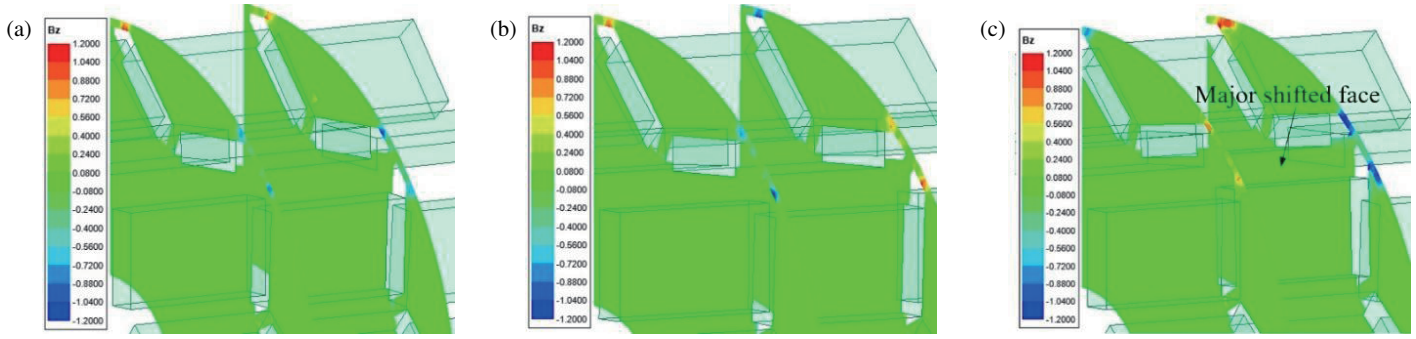

FIGURE 9. Distribution of axial magnetic density between shifted faces. (a) Linear step skew. (b) V shape skew. (c) Interchanged skew.

TABLE 3. The i-th segment rotation angle/(deg).

Segment number	Linear step	V shape	Interchanged
3	0; 2.5; 5	0; 2.5;	0; 2.5; −2.5
4	0; 1.875; 3.75; 5.625	0; 1.875; 1.875;	0; 1.875; −3.75; −1.875
5	0; 1.5; 3; 4.5; 6	0; 1.5; 3; 1.5;	0; 1.5; 3; −3; −1.5
6	0; 1.25; 2.5; 3.75; 5; 6.25	0; 1.25; 2.5; 2.5; 1.25;	0; 1.25; 2.5; −3; −2.5; −1.25

rection is opposite to that of other shifting faces. The more the number of segments is, the larger shift angle is on major shifted surface, and the more magnetic leakage is.

In order to assess the effects of the three skew modes on the motor performance at different segment numbers, 3D finite element simulation models were established. The effective value of the ideal three-phase symmetric input current was set to 55 A for every model. The corresponding motor characteristics were compared as shown in Figure 10.

It can be seen from Figure 10 that with the increase of the number of segments, the average output torque of the three skew types decreases, while the output torque of the segment interchange skew is slightly lower than that of the linear step skew. This is because the major shifted face has more magnetic leakage and loses the effective radial magnetic flux. The V shape skew has similar variation tendency, but smaller variation value.

The output torque ripple and cogging torque of all three skew types decrease with the increase of the number of segments, and the segment interchange skew is lower than that of the linear step skew. Both linear step skew and segment interchange skew have a smaller cogging torque with 4 segments than 5 segments, which is consistent with the previous analysis. Furthermore, the cogging torque of the segment interchange skew

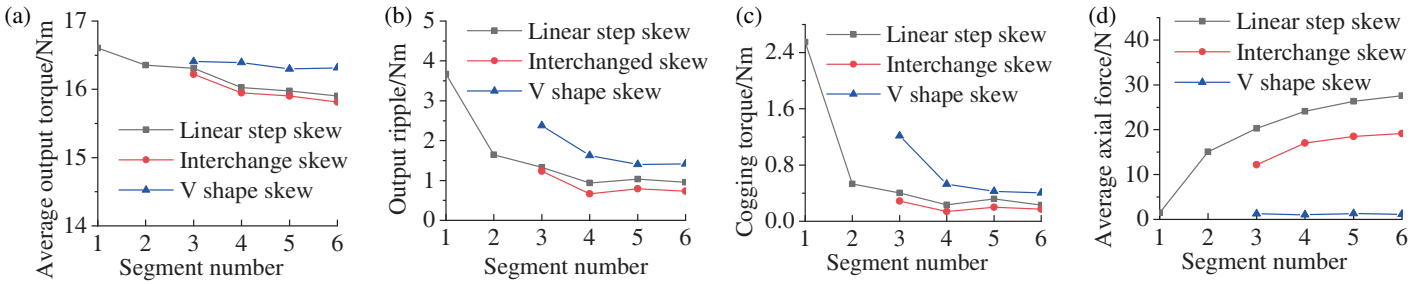

FIGURE 10. Motor characteristic comparison.

FIGURE 11. Rotor core.

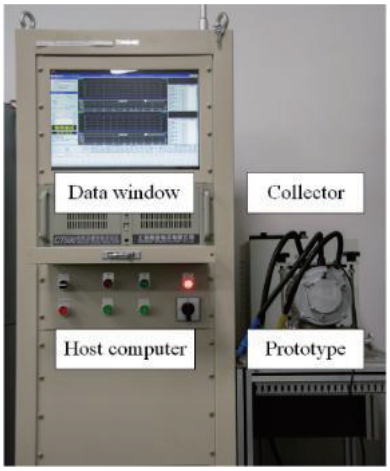

FIGURE 12. Cogging torque platform.

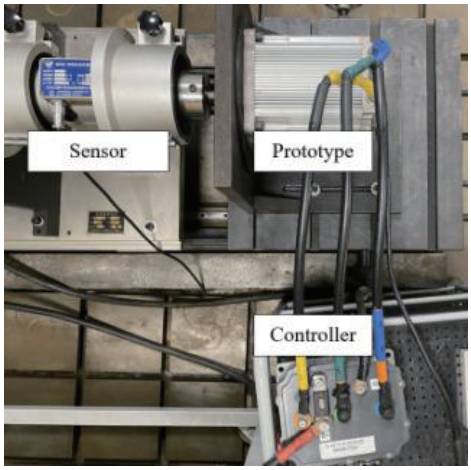

FIGURE 13. Output platform.

is smaller, due to the loss of air gap magnetic field energy storage, and more magnetic leakage in the major shifted surface. As for the V shape skew, more segments are required to achieve the weakening effect, which is difficult to be applied in motors with small radial length ratio. With the increase of the number of segments, the total angle of the skew increases; the arrangement of the skew is more and more similar to the continuous skew; and the axial force also increases. The segment interchange skew provides a leakage flux opposite to the other segments at the major shifted face, and the axial force is less than the linear step skew. The simulation results verify the above analysis of the effect of the skew pole structure on the axial force.

5. EXPERIMENT AND ANALYSIS

It can be seen from the figure that with the increase of the number of segments, the average output torque of the linear segment skew and the segment interchange skew decreases, while the output torque of the segment interchange skew pole is slightly lower than that of the linear skew pole. Experiments on cogging torque for three skew modes and non-skew methods were conducted. In the cogging torque test, the prototype machine (rotor core was shown in figure 11) and sensor are installed coaxially, and the tester drives the prototype machine to rotate, as shown in Figure 12. The test equipment adopts adaptive cancellation and decoupling separation technology and signal feature amplification technology to accurately extract the cogging torque signal from the above additional torque. All three skew modes adopt segment number as four. The comparison of cogging torque test results is shown in Figure 14. Experiments on output torque ripple under various load rates at rated speed were conducted. In the output torque test, the prototype is coaxially connected with the magnetic powder brake (as shown in Figure 13), which can provide a stable load. The output ripple at different load rates is shown in Figure 15.

The maximum range of the cogging torque testing equipment used is 2 Nm; the minimum torque measurement division is 0.5 mNm; and the minimum resolution angle is 0.1 deg. The test rotation speed range is 1 rpm–20 rpm. Due to the limitations in the 3D simulation accuracy of the simulation software, along with prolonged simulation times, there are disparities between the actual test results and simulation results. However, it is noteworthy that the overall torque variation range is essentially consistent. The linear step skew cogging torque peak difference of the simulation results is 138 mNm, while the experimentally measured peak difference is 158 mNm. Meanwhile, the experimentally measured cogging torque of V shape skew is 536 mNm, and linear step skew is 183 mNm.

Through a comparative analysis of the output ripple and cogging torque at rated condition in Figure 15, it can be seen that the cogging torque constitutes the main component in the output ripple. Furthermore, by comparing the torque ripples of different skewing methods under various load rates, it is evident that

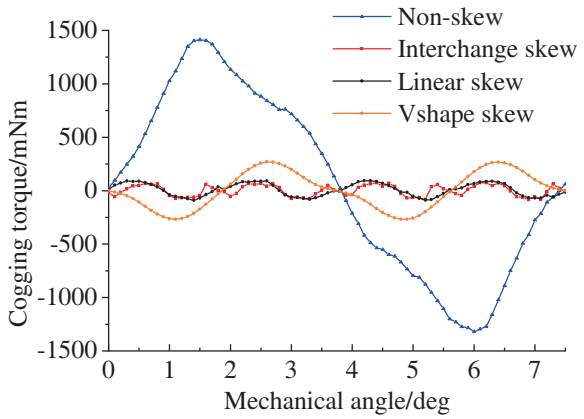

FIGURE 14. Comparison of cogging torque.

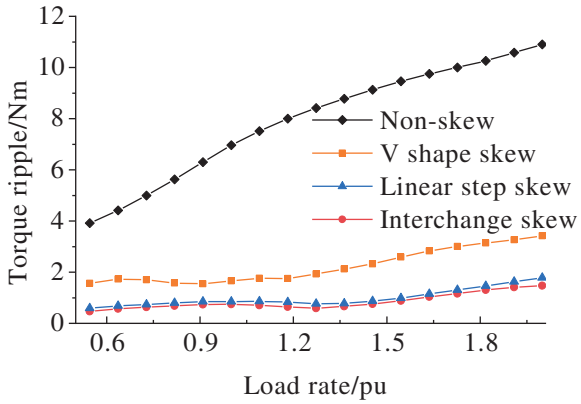

FIGURE 15. Output ripple at different load rate.

employing skewing can effectively suppress the output ripple. The output ripple increases with the rise in load rate, and the ripple rises slower with linear segmentation or interchange of segments, than V shape skew. In addition, the linear step skew and interchange skew have minimum ripple around 1.2 pu of the rated load, and the V shape skew has minimum ripple around 0.9 pu of the rated load. Finally, in all three skew modes, the interchange skew has the smallest ripple.

The experimental results support the analysis that after adopt interchange skew and the rotor is divided into four segments, the cogging torque peak difference of the motor is reduced from the original 2.55 Nm to 158 mNm. This shows that the segment skew pole structure can indeed effectively reduce the cogging torque, which verifies the results obtained from the simulation.

6. CONCLUSIONS

Based on the hypothesis analysis of the general slot torque, the period of the cogging torque is derived. Then, based on Fourier series, the relationship between the number of rotor segments and the subharmonic of the slot torque is derived. The whole section analysis only uses mathematical method, and the derivation process is simple and has wide applicability. By analysing the source of axial force when the rotor skew pole is segmented, a new segmented method is proposed, which can effectively reduce the axial force produced when the rotor adopted interchange skew.

The experiment demonstrates that interchanged skew can achieve a cogging torque reduction level similar to that of linear step skew. The cogging torque, after the application of interchanged skew, decreased from the original 2.55 Nm to 158 mNm. In addition, compared to linear step skew, interchanged skew exhibits smaller output torque ripple, which is beneficial for the output performance of the motor.

REFERENCES

[1] Nian, S., L. Zhu, X. Luo, and Z. Huang, "Analytical methods for optimal rotor step-skewing to minimize cogging torque in permanent magnet motors," in *2019 22nd International Conference on Electrical Machines and Systems (ICEMS)*, 2019.

[2] Zhang, S. S. and S. Y. Guo, "Analytical magnetic field method of permanent magnet synchronous machine considering step-skewed magnets and magnetic slot wedge," *Transactions of China Electrotechnical Society*, Vol. 34, No. 01, 11–22, 2019.

[3] Kim, K.-C., "A novel method for minimization of cogging torque and torque ripple for interior permanent magnet synchronous motor," *IEEE Transactions on Magnetics*, Vol. 50, No. 2, 793–796, 2014.

[4] Luo, H. and Z. Liao, "Harmonic analysis and minimization of cogging torque in permanent magnet motors," *Electric Machines and Control*, Vol. 14, No. 4, 36–40, 2010.

[5] Dutta, R., K. Ahsanullah, and F. Rahman, "Cogging torque and torque ripple in a direct-drive interior permanent magnet generator," *Progress In Electromagnetics Research B*, Vol. 70, 73–85, 2016.

[6] Zhang, J.-C., X.-Y. Huang, Y.-T. Fang, and Z.-K. Ma, "Design of interior PM synchronous traction motor with novel approximate skewed rotor," in *IECON 2012 — 38th Annual Conference on IEEE Industrial Electronics Society*, 1726–1730, 2012.

[7] Xu, K., H.-L. Ying, S.-R. Huang, *et al.*, "Electromagnetic noise reduction of permanent magnet synchronous motor by step-skewed rotor," *Journal of Zhejiang University (Engineering Science)*, Vol. 53, No. 11, 2248–2254, 2019.

[8] Gao, M., X. Yang, S. Jiang, *et al.*, "The method for reducing cogging torque by suitable selection of the pole-arc coefficient and rotor step skewing in five-phase permanent magnet motor," *Proceedings of the CSEE*, 1–12, 2023.

[9] Yang, Y., X. Wang, X. Chen, and P. Ji, "A method for reducing cogging torque by different slot widths in permanent magnet motors," *Transactions of China Electrotechnical Society*, Vol. 20, No. 3, 40–44, 2005.

[10] Zang, J., Y. Wang, and L. Jing, "A method of reducing air-gap harmonic of permanent magnet motor for fitness car," *Progress In Electromagnetics Research Letters*, Vol. 83, 37–44, 2019.

[11] Dhulipati, H., S. Mukundan, K. L. V. Iyer, and N. C. Kar, "Skewing of stator windings for reduction of spatial harmonics in concentrated wound PMSM," in *2017 IEEE 30th Canadian Conference on Electrical and Computer Engineering (CCECE)*, Windsor, ON, Canada, 2017.

[12] Fei, W., P. C. K. Luk, and J. Shen, "Torque analysis of permanent-magnet flux switching machines with rotor step skewing," *IEEE Transactions on Magnetics*, Vol. 48, No. 10, 2664–2673, 2012.

[13] Ocak, O. and M. Aydin, "An innovative semi-FEA based, variable magnet-step-skew to minimize cogging torque and torque pulsations in permanent magnet synchronous motors," *IEEE Access*, Vol. 8, 210 775–210 783, 2020.

[14] Rashid, M. K. and A. M. Mohammed, "Elimination of cogging torque and torque ripple in magnetic gear using slicing technique," *Progress In Electromagnetics Research C*, Vol. 125, 179–189, 2022.

[15] Blum, J., J. Merwerth, and H.-G. Herzog, "Investigation of the segment order in step-skewed synchronous machines on noise and vibration," in *2014 4th International Electric Drives Production Conference (EDPC)*, Nuremberg, Germany, 2014.

[16] Islam, R., I. Husain, A. Fardoun, and K. Mclaughlin, "Permanent-magnet synchronous motor magnet designs with skewing for torque ripple and cogging torque reduction," *IEEE Transactions on Industry Applications*, Vol. 45, No. 1, 152–160, 2009.

[17] Kang, C. H., K. J. Kang, J. Y. Song, Y. J. Cho, and G. H. Jang, "Axial unbalanced magnetic force in a permanent magnet motor due to a skewed magnet and rotor eccentricities," *IEEE Transactions on Magnetics*, Vol. 53, No. 11, 1–5, 2017.

[18] Jiang, J. W., B. Bilgin, Y. Yang, A. Sathyan, H. Dadkhah, and A. Emadi, "Rotor skew pattern design and optimisation for cogging torque reduction," *IET Electrical Systems in Transportation*, Vol. 2, No. 6, 126–135, 2016.

[19] Ran, H., L. Wu, W. Bai, J. Zhao, and Y. Liu, "Multi-objective optimization and analysis of a novel permanent magnet synchronous motor," *Progress In Electromagnetics Research C*, Vol. 138, 13–26, 2023.

[20] Jing, L., J. Gong, and Y. Lin, "Analysis and reduction of cogging torque of line-start permanent magnet motors," *Progress In Electromagnetics Research M*, Vol. 78, 115–124, 2019.

[21] Yan, S., X. Zhang, Z. Gao, M. Xu, L. Wang, Y. Zhang, W. Zhang, and K. Geng, "Research on the built-in tangential and radial combined-pole permanent magnet hub drive motor for electric vehicles," *Progress In Electromagnetics Research C*, Vol. 124, 253–267, 2022.

[22] Jing, L., J. Chen, Z. Huang, and J. Gong, "Exact analytical method for air-gap main magnetic field computation and cogging torque of SMPM motors," *Progress In Electromagnetics Research M*, Vol. 81, 75–84, 2019.

[23] Luo, H. H. and Z. L. Liao, "Harmonic analysis and minimization of cogging torque in permanent magnet motors," *Electric Machines and Control*, Vol. 14, No. 4, 36–40+45, 2010.

[24] Zhu, Z. Q. and D. Howe, "Influence of design parameters on cogging torque in permanent magnet machines," *IEEE Access*, Vol. 15, No. 4, 407–412, 2002.

[25] Zhu, L., S. Z. Jiang, Z. Q. Zhu, and C. C. Chan, "Analytical methods for minimizing cogging torque in permanent-magnet machines," *IEEE Transactions on Magnetics*, Vol. 45, No. 4, 2023–2031, Apr. 2009.

[26] Reza, M. M. and R. K. Srivastava, "Cogging reduction in permanent magnet machines via skewed slot opening and its analytical modeling," *Progress In Electromagnetics Research M*, Vol. 70, 167–176, 2018.

[27] Baolai, L., "Calculation method for axial force of motor based on two-dimensional electromagnetic field simulation," *Micromotors*, Vol. 52, No. 8, 6, 2019.

[28] Zhao, W., T. A. Lipo, and B. I. Kwon, "Torque pulsation minimization in spoke-type interior permanent magnet motors with skewing and sinusoidal permanent magnet configurations," *IEEE Transactions on Magnetics*, Vol. 51, No. 11, 1–4, 2015.

[29] Lin, H., Q. Zhang, and S. Huang, "Analysis of axial electromagnetic force in permanent magnet synchronous motor with rotor shift step skewing," *Small & Special Electrical Machines*, Vol. 49, No. 03, 6–10, 2021.

[30] Ge, X., Z. Q. Zhu, G. Kemp, D. Moule, and C. Williams, "Optimal step-skew methods for cogging torque reduction accounting for three-dimensional effect of interior permanent magnet machines," *IEEE Transactions on Energy Conversion*, Vol. 32, No. 1, 222–232, Mar. 2017.

[31] Ying, H., Z. Y. Zhang, J. Q. Qu, and S. R. Huang, "Application of step skewing to permanent magnent synchronous motors," *Small and Special Electrical Machines*, Vol. 37, No. 7, 10–14, 2009.

[32] Jin, M., W. Fei, and J. Shen, "Investigation of axial magnetic force in permanent magnet synchronous machines with rotor step skewing," *Transactions of China Electrotechnical Society*, Vol. 28, No. 11, 19–27, 2013.